Myocardial Contractile Reserve and Perfusion Defect Severity with Rest and Stress Dobutamine ^{99m}Tc-Sestamibi SPECT in Canine Stunning and Subendocardial Infarction

Bennett B. Chin, MD[1]; Giuseppe Esposito, MD[2]; and Dara L. Kraitchman, VMD, PhD[1]

[1]Russell H. Morgan Department of Radiology and Radiological Science, Johns Hopkins Medical Institutions, Baltimore, Maryland; and [2]Centro di Studio per la Medicina Nucleare, CNR, Naples, Italy

Myocardial contractile reserve and resting perfusion scintigraphy provide independent information to assess myocardial viability. The purpose of this study was to simultaneously evaluate both with ^{99m}Tc-sestamibi SPECT and low-dose dobutamine in canine stunning and subendocardial infarction (SEMI). **Methods:** Eighteen dogs were included in the study: 7 normal, 7 stunned, and 4 with SEMI. Closed-chest stunning and SEMI were produced by angioplasty balloon occlusion of the left anterior descending artery (20 and 90 min, respectively). Subsequent radiolabeled mircospheres confirmed reflow, and ^{99m}Tc-sestamibi was then administered at rest. Gated SPECT and MRI tagging were performed at rest and during low-dose dobutamine infusion (5 μg/kg/min). SPECT systolic wall thickening index (SWI) and MRI radial strain quantified myocardial contraction. Postmortem 2,3,5-triphenyltetrazolium chloride staining quantified SEMI. **Results:** Defect severity by SPECT in the anterior wall was mild and was not statistically different for the stunned versus SEMI groups (P = not significant). At rest, anterior wall SPECT SWI was significantly higher in the normal versus stunned groups (21.1 ± 3.1 vs. 10.1 ± 9.0; P = 0.0002) and the normal versus SEMI groups (21.1 ± 3.1 vs. 2.6 ± 6.0; P = 0.000002). With low-dose dobutamine, SWI increased significantly compared with rest for the stunned group (29.1 ± 10.4 vs. 10.1 ± 9.0; P = 0.000007) but did not increase significantly for the SEMI group (11.0 ± 11.3 vs. 2.6 ± 6.0; P = 0.09); SWI during low-dose dobutamine infusion for the stunned group was comparable to that for the normal group (29.1 ± 10.4 vs. 28.2 ± 7.0; P = 0.80). SWI also showed correlation with MRI radial strain (r = 0.42; P = 0.00015). **Conclusion:** Defect severity for stunned myocardium and SEMI was mild and was not significantly different. Contractile reserve was significantly different in stunned myocardium and SEMI. ^{99m}Tc-Sestamibi SPECT at rest and with low-dose dobutamine is a promising new technique to simultaneously assess myocardial perfusion and contractile reserve.

Myocardial viability, defined as improvement in wall motion after revascularization, may be assessed by techniques indicating myocyte cell membrane integrity or myocardial contractile reserve. Maintenance of cell membrane integrity may be assessed through metabolic processes including Na^+-K^+ adenosinetriphosphatase activity, an intact electrochemical gradient across the cell membrane, or preservation of fatty acid or glucose metabolism as defined by radiotracer techniques (^{201}Tl chloride, ^{99m}Tc-sestamibi, ^{123}I-β-methyl-p-iodophenylpentadecanoic acid, ^{18}F-FDG PET). These radiotracer techniques, which evaluate whether viable myocytes are present, may also overestimate functional recovery after revascularization because of myocardial fibrosis (1–5). A potential disadvantage of radiotracer techniques is the limited spatial resolution in which mild severity defects attributed to subendocardial infarction (SEMI) may be difficult to distinguish from stunned or hibernating myocardium.

Other techniques that evaluate myocardial contractile reserve, such as dobutamine echocardiography, have high positive predictive value for functional improvement but may underestimate viability if coronary flow reserve is impaired (3–5). Without an adequate coronary flow reserve, the contractile response may be decreased or absent, and such a territory could potentially be misclassified as nonviable (6). Although a biphasic response of initial improvement followed by worsening contractility shows high specificity for viability, this response has a relatively low sensitivity (3–5). In the absence of contractile reserve, but in the presence of resting perfusion radiotracer uptake, the demonstration of ischemia by perfusion scintigraphy could further identify regions that may represent viable myocar-

dium. Perfusion scintigraphy, when used as a conventional stress and rest comparison study to assess coronary flow reserve, may identify viable myocardium by delineating areas of myocardial ischemia (*7*).

When combining indices of coronary flow reserve with cellular viability by perfusion scintigraphy, the positive and negative predictive values have been reported to be highest when both criteria are concordant (*8*). Echocardiographic coronary flow reserve and cellular viability data are also most predictive when these criteria are concordant (*9*). Thus, the complementary data derived from myocyte membrane integrity, myocardial contractile reserve, and coronary flow reserve may better identify viable myocardium than any single test alone.

^{99m}Tc-Sestamibi is a single photon tracer that permits the assessment of myocyte membrane integrity as well as the potential to assess contractile reserve. Its ability to assess coronary flow reserve, as a conventional stress and rest perfusion scintigraphic study, is well established. The purpose of this study was to characterize measurements of myocyte membrane integrity and contractile reserve in a canine model of stunning and SEMI to evaluate the potential of this new technique to identify viable myocardium.

MATERIALS AND METHODS

Animal Preparation

All animal studies were approved by the Institutional Animal Care and Use Committee and adhered to the American Veterinary Medical Association guidelines. Twenty mongrel dogs (22–25 kg) were fasted and then sedated (intramuscular atropine, 0.05 mg/kg; xylazine, 2.5 mg/kg; and ketamine, 5 mg/kg), intubated, and placed under general inhalation anesthesia (1%–2% isoflurane). Seven dogs were normal controls and 7 underwent stunning. In the SEMI group, only 4 of 6 were included in the analysis because of a large transmural myocardial infarction in 1 dog and a nonreperfused infarction in another.

For coronary artery occlusion, an angioplasty balloon catheter (Cordis, Diamond Bar, CA) was guided by fluoroscopy into the proximal left anterior descending coronary artery (LAD). The balloon was inflated for 20 min and subsequently removed to produce stunning; a longer time (90 min) of occlusion followed by reperfusion was used to produce SEMI. Standard radiolabeled microsphere techniques measured myocardial blood flow at baseline, during occlusion, and 15 min after reperfusion. Lidocaine (1 mg/kg/min) was administered to minimize arrhythmias, and 5,000 IU heparin were given intravenously to minimize thrombosis. After balloon deflation and reflow, monitoring was performed for cardiac arrhythmias and hypotension for at least 15 min. After stabilization and transfer from the catheterization laboratory to the imaging suite, ^{99m}Tc-sestamibi (27.75–37 MBq/kg [0.75–1.0 mCi/kg]) was administered intravenously.

MRI Acquisition

A 1.5-T MR scanner (General Electric Medical Systems, Milwaukee, WI) was used with a phased-array transmit–receive surface coil. Multiphase, short-axis, and long-axis tagged images were obtained using a cardiac-gated, breathhold segmented k-space fast spoiled gradient-echo pulse sequence: repetition time/

echo time = 6.2/1.2 ms; 12° flip angle; 128 × 256 matrix interpolated to 256 × 256; 7- to 10-mm slice thickness; 28-cm field of view; 1 to 2 signal averages; 4–8 k-space lines per segment; 6 mm tag-to-tag spacing; and 32-kHz bandwidth. A 2-dimensional tagging grid was used in the short-axis images and 1-dimensional grids were used in the long axes. Afterward, dobutamine (5 μg/kg/min intravenously) was infused continuously and the imaging sequences were repeated.

SPECT Acquisition

Gated SPECT was acquired on a 3-detector system (Triad; Trionix, Twinsburg, OH) in a 64 × 64 matrix, pixel size = 0.36 cm^3 per voxel, with projection data acquired at each 3° over a 360° rotation. Gating was acquired in 8 time frames per cardiac cycle with 40–60 beats per projection. The acquisition was then repeated during infusion of low-dose dobutamine (5 μg/kg/min). Images were reconstructed with 360° data and filtered backprojection with a low-pass Hanning filter (4.0 rolloff) cutoff frequency of 0.45 cycle/cm (0.65 cycle/cm for nongated data). The 360° reconstruction was used to decrease any potential variability caused by the more midline orientation of the canine left ventricular myocardium. No scatter correction or attenuation correction was applied. The nongated SPECT was generated by summing all 8 raw-time projection data followed by filtered backprojection reconstruction. MRI and SPECT images were acquired in a random order. All imaging of myocardial stunning was performed within the first hours of myocardial stunning.

Ex Vivo Validation

After each animal was euthanized, the heart was excised and sectioned along the short axis. Within 6 h of reperfusion, tissue was incubated in 2% 2,3,5-triphenyltetrazolium chloride (TTC) for 20 min at 37°C and then photographed with a digital camera for analysis. The area of SEMI was defined as the nonstaining region with TTC. After formalin fixation, sectioning, and weighing, samples were counted in a γ-emission well spectrometer (model 5986; Hewlett Packard, Andover, MA) along with reference blood samples. Regional myocardial blood flow was calculated using standard techniques (*10*).

MRI Analysis

The MRI tag lines were first detected and tracked. From these, 3-dimensional motion and strains were calculated using a field-fitting technique (*11*). The 3-dimensional strains were determined on a regional basis (*12*) at rest and during dobutamine infusion. The midwall systolic radial normal (or radial thickening) strains were compared with their corresponding regions in the gated SPECT studies.

SPECT Analysis

SPECT defect severity was obtained with circumferential profiles in the short-axis view at the midventricular level. Myocardial activity was normalized to the anterolateral wall because of varying degrees of high liver activity. Defect severity was defined as the percentage of this normalized activity. Systolic wall thickening index (SWI) was calculated as SWI = (end systole − end diastole)/end systole$_{max}$ · 100, where end systole$_{max}$ is defined as the maximum count activity of the 8 time-frame gated volume dataset (the anterolateral wall intensity in end systole at 135°). Our definition of SWI with end systole$_{max}$ in the denominator differs from that of earlier authors (*13*), who use the end-diastolic value. The rationale in using a single maximum value for normalization of

count intensity includes (a) avoidance of a region-specific end-diastolic value in the denominator, which eliminates the tendency of SWI to be relatively increased in regions of defects (i.e., in defects, the lower end-diastolic value in the denominator increases the overall SWI compared with using a higher single end systole$_{max}$ for all SWI measurements); (b) SWI in normal remote areas and SWI in normal controls is more meaningful for comparison purposes with abnormal (stunned or infarcted); and (c) use of a maximum count intensity decreases the variability in the measurement because it is less subjective compared with other methods that may use different criteria for choosing a single end-diastolic value.

For wall motion comparisons, gated MRI and gated SPECT short-axis data were reoriented by visual alignment of the septum, right ventricle, base, and apex. The most basal SPECT slices were excluded from SWI analysis because of the normal decreased activity of the basal septal region. The 0° angle was defined as the midinferior wall, the 90° angle was defined as the lateral wall, and the 180° angle was defined as the midanterior wall.

Infarct Quantification

Digital images of TTC-stained short-axis slices were analyzed with a Scion Image software package (Scion Corp., Frederick, MD). For each slice, regions of interest were drawn to define the entire left ventricular area and the infarct area. The percentage of infarcted area (%MI) was calculated by dividing the infarcted area by the corresponding short-axis area. The %MI was used for correlation analysis with the corresponding SWI values.

Statistical Analysis

Continuous data were expressed as mean ± 1 SD. Statistical comparisons for significant differences between groups (normal, stunned, and SEMI) were evaluated with the 2-tailed Student t test. Comparisons within groups were evaluated with the paired 2-sample Student t test. Simple linear regression analysis was used for correlations of MRI radial strain with SPECT SWI and for correlations of %MI with SWI values.

RESULTS

Defect Severity

Overall, the average defect severity was mild for stunned ($n = 7$) and SEMI ($n = 4$) groups; both groups showed considerable overlap when compared with the normal ($n = 7$) group. This was true for nongated, gated end-diastolic, and gated end-systolic images. Table 1 summarizes defect severity in nongated and gated images at baseline and with dobutamine for all groups. Figure 1 shows a comparison of the mean defect severity in each group.

Defect severity was similar for the stunned group compared with the SEMI group and no statistically significant differences were found. No significant differences were found in the stunned group versus the SEMI group in nongated baseline ($P = 0.78$), nongated dobutamine ($P = 0.40$), gated end-diastolic baseline ($P = 0.64$), gated end-systolic baseline ($P = 0.84$), gated end-diastolic dobutamine ($P = 0.82$), and gated end-systolic dobutamine ($P = 0.29$).

In the stunned group, defect severity compared with the normal group was statistically different in resting gated end-systolic images only ($P < 0.03$). No significant differences were found between the stunned and normal groups for nongated baseline ($P = 0.27$), nongated dobutamine ($P = 0.50$), gated end-diastolic baseline ($P = 0.30$), gated end-diastolic dobutamine ($P = 0.70$), and gated end-systolic dobutamine ($P = 0.29$).

In the SEMI group, defect severity compared with that of the normal group was statistically different only on resting gated end-systolic images ($P < 0.05$). No significant differences were found between SEMI and normal for nongated baseline ($P = 0.31$), nongated dobutamine ($P = 0.23$), gated end-diastolic baseline ($P = 0.27$), gated end-diastolic dobutamine ($P = 0.51$), and gated end-systolic dobutamine ($P = 0.36$).

Gated Wall Motion–SWI

In all stunning and infarction cases, the resting tagged MRI showed decreased myocardial strain in the regions subtended by the occluded LAD. The results for SWI are summarized in the Tables 2 and 3. The SWI at rest and during dobutamine infusion for all groups is summarized in Figure 2. At baseline, SWI in the anterior wall was significantly higher for the normal group compared with that of

TABLE 1
Defect Severity: Anterior Wall

Group	Nongated		Rest		Dobutamine	
	Rest	Dobutamine	End diastolic	End systolic*	End diastolic	End systolic
Normal	95.2 ± 14.3 (80.5–115.2)	96.8 ± 8.8 (84.1–111.1)	95.6 ± 10.3 (82.01–110.6)	98.3 ± 8.6 (87.1–110.6)	99.0 ± 12.7 (82.0–113.3)	98.0 ± 5.1 (91.5–104.4)
Stunned	88.1 ± 7.6 (75.9–97.8)	93.9 ± 6.7 (83.7–102.1)	90.8 ± 6.0 (82.8–102.4)	89.4 ± 4.2 (85.2–97.6)	92.5 ± 8.8 (79.3–107.4)	99.2 ± 6.6 (88.8–106.8)
SEMI	90.4 ± 6.4 (82.0–96.3)	91.9 ± 2.7 (89.5–95.2)	89.2 ± 3.4 (86.1–93.3)	89.9 ± 3.6 (85.9–94.3)	93.9 ± 10.9 (78.6–104.0)	95.3 ± 2.3 (92.3–97.3)

*At rest in end systole: normal vs. stunned (98.3 ± 8.6 vs. 89.4 ± 4.2; $P < 0.03$) and normal vs. SEMI (98.3 ± 8.6 vs. 89.9 ± 3.6; $P < 0.05$) were significantly different. All other comparisons of defect severity between groups did not reach statistical significance ($P =$ not significant).

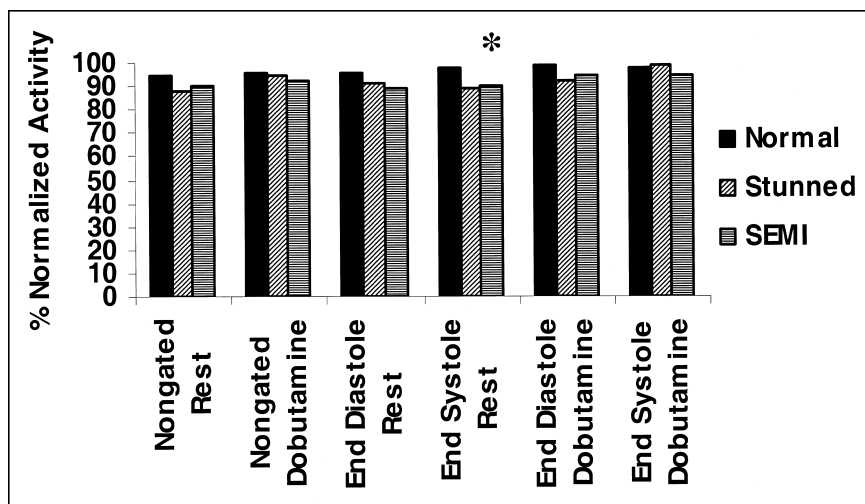Data are expressed as mean ± 1 SD with range in parentheses.

FIGURE 1. Defect severity in nongated and gated end-diastolic and gated end-systolic tomographic images. Asterisk indicates significant differences in resting end-systolic images: normal vs. stunned ($P < 0.03$) and normal vs. myocardial infarction ($P < 0.05$).

the stunned group ($P = 0.0002$); SWI was also higher for the normal group compared with that of the SEMI group ($P = 0.000002$). At baseline, the mean SWI for the stunned group was higher than that for the SEMI group ($P = 0.03$).

During dobutamine infusion, the SWI was significantly higher in the normal group compared with that of the SEMI group ($P = 0.003$); the SWI was also significantly higher in the stunned group compared with that of the SEMI group ($P = 0.002$). The SWI during dobutamine infusion was not significantly different in the normal group compared with that of the stunned group ($P = 0.80$).

During dobutamine infusion, the SWI in the normal group increased significantly compared with that of the baseline group ($P = 0.003$); the SWI for the stunned group also increased significantly compared with that of the baseline group ($P = 0.000007$). However, during dobutamine infusion, the SWI for the SEMI group did not increase significantly ($P = 0.09$). The mean increase in SWI after dobutamine infusion for the stunned group was significantly greater than that for the SEMI group ($P = 0.05$). The mean increase in SWI after dobutamine infusion was also significantly greater for the stunned group compared with that of the normal group ($P = 0.001$).

Examples of short-axis midventricular SPECT images and data analysis are shown for the normal, stunned, and

SEMI groups in Figures 3, 4, and 5, respectively. The anterior wall is in the 180° orientation. High liver activity is present in the regions of 0° and 360° and limits the interpretation of SWI in this region.

Correlation of SWI with MRI Radial Strain

The SWI measurements by SPECT correlated with MRI radial strain measurements in the anterior ($r = 0.5$; $P = 0.009$) and anterolateral ($r = 0.44$; $P = 0.02$) walls. The measurements in the septum correlated poorly with MRI radial strain ($r = 0.26$; $P =$ not significant) The inferior and inferolateral areas could not be quantified by SPECT because of the high and variable liver activity. Figure 6 shows the overall correlation of SWI determined from SPECT with MRI radial strain in the anterior and anterolateral walls. In all cases of stunning and SEMI, the resting tagged MRI showed decreased myocardial strain in the regions subtended by the occluded LAD. With dobutamine loading, recruitable myocardial function was shown on a segmental basis in the LAD bed of stunned animals. By contrast, recruitable myocardium could not be found in subendocardial infarcted myocardium.

TABLE 2
SWI (%): Contractile Reserve

Group	Rest	Dobutamine	Change	P
Normal	21.1 ± 3.1 (20.1–25.2)	28.2 ± 7.0 (16.1–40.5)	6.1 ± 5.8 (−4.4–15.3)	0.003
Stunned	10.1 ± 9.0 (−1.4–25.8)	29.1 ± 10.4 (12.5–37.8)	18.9 ± 9.9 (6.6–38.5)	0.000007
SEMI	2.6 ± 6.0 (−6.5–10.5)	11.0 ± 11.3 (−1.9–26.4)	6.9 ± 12.5 (−6.7–25.1)	0.11

Data are expressed as mean ± 1 SD with range in parentheses.

TABLE 3
SWI (%): Comparisons Between Groups

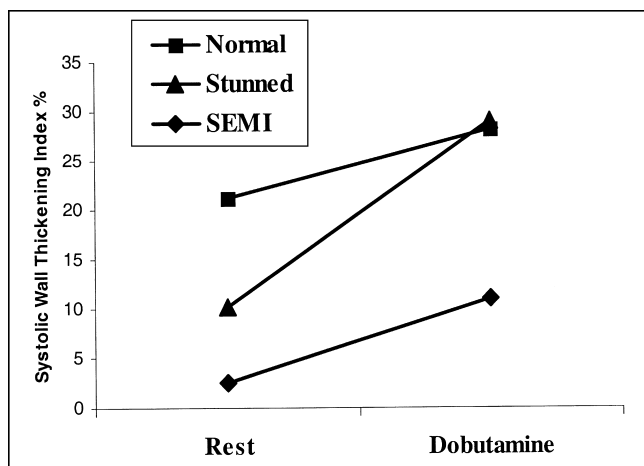| Group			P
Rest			
Normal vs. stunned	21.1 ± 3.1	10.1 ± 9.0	0.0002
Normal vs. SEMI	21.1 ± 3.1	2.6 ± 6.0	<0.000001
Stunned vs. SEMI	10.1 ± 9.0	2.6 ± 6.0	0.046
Dobutamine			
Normal vs. stunned	28.2 ± 7.0	29.1 ± 10.4	0.93
Normal vs. SEMI	28.2 ± 7.0	11.0 ± 11.3	0.0007
Stunned vs. SEMI	29.1 ± 10.4	11.0 ± 11.3	0.001

Data are expressed as mean ± 1 SD.

FIGURE 2. SWI at baseline and during dobutamine infusion.

Correlation of SWI and Defect Severity with Infarct Size by TTC

The mean size of the SEMI %MI was 7.2% ± 2.2% (range, 4.37%–9.09%; $n = 4$). No significant correlation was found between percentage of infarct size and SWI at rest (%MI = 0.214 · (rest SWI) + 6.2031; $r^2 = 0.5429$; $P =$ not significant) or during dobutamine infusion (%MI = −0.1285 · (SWI dobutamine) + 8.6235; $r^2 = 0.6341$; $P =$ not significant). A trend of linear inverse correlation of average infarct size versus change in SWI was seen with dobutamine (%MI = −0.1271 · (SWI dobutamine − SWI rest) + 8.0036; $r^2 = 0.9497$; $P = 0.03$). No significant correlations were found between infarct size and defect severity at rest (%MI = 0.0112 · (defect severity) + 6.2045; $r^2 = 0.001$; $P =$ not significant) and between infarct size and defect severity during dobutamine infusion (%MI = 0.6808 · (defect severity) − 55.343; $r^2 = 0.705$; $P =$ not significant).

DISCUSSION

In patients with coronary artery disease and left ventricular dysfunction, myocardial viability assessment is an important prognostic determinant of postoperative functional improvement, future ischemic events, and cardiac mortality (*14–16*). Several studies have shown good results for viability measurement techniques that evaluate myocyte membrane integrity or contractile reserve. In a comparison of both approaches, the presence of resting perfusion has shown a higher sensitivity but a lower specificity for improvement in wall motion after revascularization compared with techniques that evaluate contractile reserve (*3–5,17,18*). Although the individual test sensitivity and specificity can be altered by changing the threshold for defining criteria, the highest positive and negative predictive values have been obtained when information from both criteria are concordant (*8,9*), suggesting that the combination of techniques may be more accurate than a single test alone.

Mild defects on scintigraphy may be a result of myocardial stunning, SEMI, a true decrease in resting perfusion, or

an imaging artifact. In this study, resting perfusion was restored after myocardial reflow that was subsequently confirmed by using radioactive microspheres. Akinesis or hypokinesis in stunned myocardium with less than normal wall thickening may result in a lower detected SPECT activity because of the partial-volume effect (*19*). Mild defects from stunned or hibernating myocardium may be difficult to distinguish from SEMI with fibrosis on the basis of resting perfusion scintigraphy (*4,7,8*). In addition, several other imaging factors influence defect severity. Photon attenuation has also been implicated as a cause of lower accuracy in assessing viability, especially in the inferior wall (*20,21*). Conversely, limited spatial and temporal resolution, translational and rotational motion during myocardial contraction, and respiratory motion may result in underestimation of defect severity.

Because defect severity may be influenced by differences in the partial-volume effect attributed to wall motion abnormalities, this study examined defect severity in end diastole, in end systole, and on the nongated images at rest and during dobutamine infusion. In these canine models of stunning and SEMI, mild severity defects were present on gated and nongated images. The only statistically significant differences in defect severity occurred at rest during end systole when comparing normal versus stunned groups and normal versus SEMI groups. Because the highest detected counts in normally contracting segments occur in end systole, the highest contrast between normal and abnormal segments also occurs at end systole. The absence of a significant difference during dobutamine infusion could be caused by cardiac motion and limited temporal resolution. Also, the mean percentage of the midventricular slice with SEMI was approximately 7%; therefore, the total extent of infarction was relatively small. Overall, mild severity defects were present in SEMIs and stunned myocardium, and the difference in defect severity was not statistically significant.

These findings are in agreement with the clinical observation that not all mild-to-moderate severity resting scintigraphic defects will improve with revascularization. A SEMI resulting in a mild severity resting perfusion defect is less likely to improve after revascularization. A previous study showed only 33% improvement in wall motion in mild-to-moderate severity irreversible defects in patients compared with an 83% recovery in those that showed reversibility by ^{201}Tl exercise-redistribution-reinjection SPECT scintigraphy (*7*). Although both groups showed a similar defect severity, resting thallium defect by quantification, an improvement in wall motion after revascularization was less likely without evidence of concurrent ischemia. This observation supports the hypothesis that mild resting severity defects may be present in SEMIs, in areas of viability that may be stunned and showing incomplete redistribution, or in hibernating myocardium.

When defining myocardial viability on the basis of improvement in wall motion after revascularization, resting
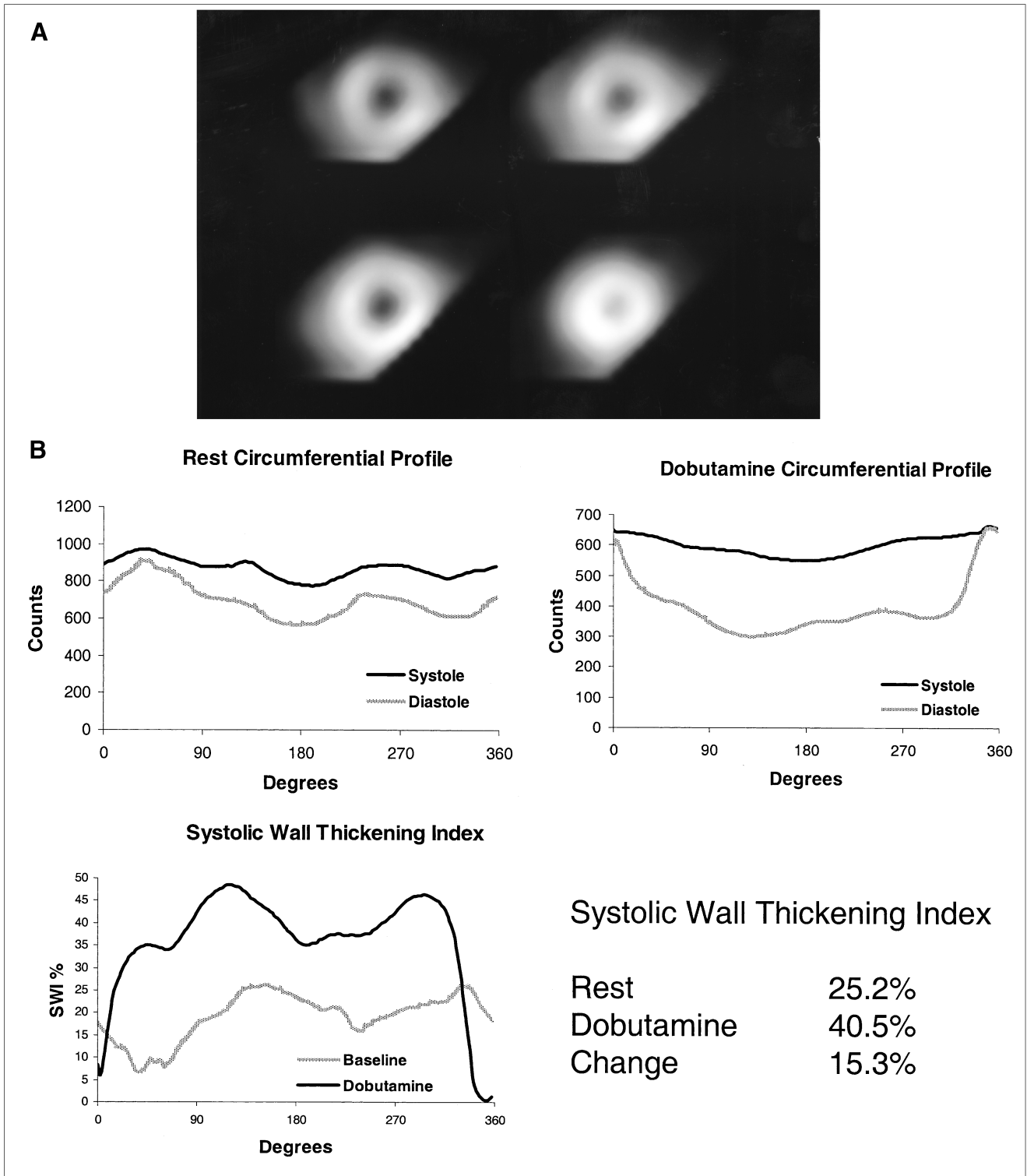
FIGURE 3. Normal (healthy) control. (A) Short-axis midventricular SPECT slices. (Top) Resting end-diastolic (left) and resting end-systolic (right) images. (Bottom) Dobutamine end-diastolic (left) and dobutamine end-systolic (right) images. (B) SPECT analysis. (Top) Circumferential profiles of midventricular short-axis slice at rest (left) and during dobutamine infusion (right). (Bottom) Percentage SWI at rest and during dobutamine infusion.
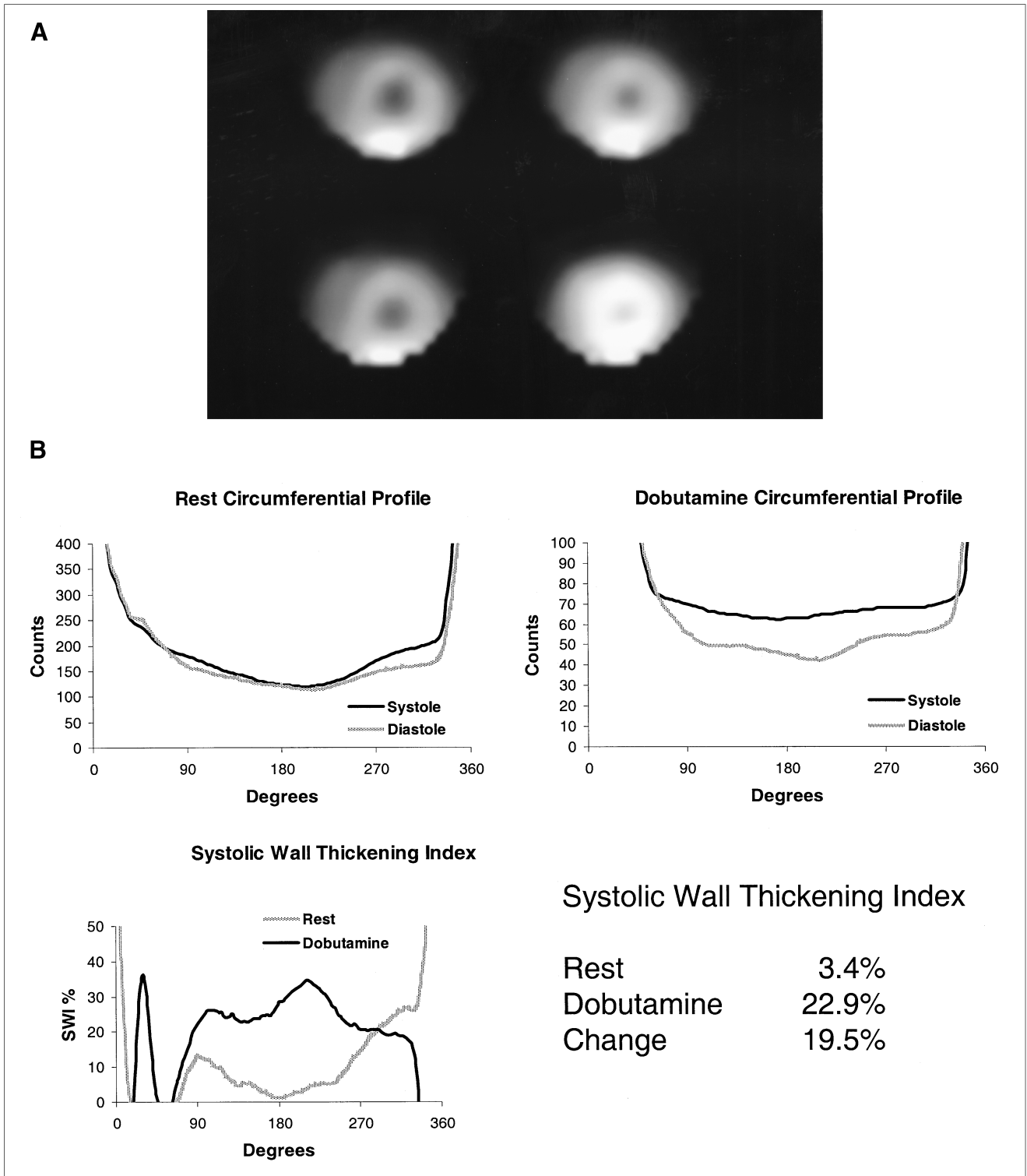
FIGURE 4. Stunned myocardium. (A) Short-axis midventricular SPECT slices. (Top) Resting end-diastolic (left) and resting end-systolic (right) images. (Bottom) Dobutamine end-diastolic (left) and dobutamine end-systolic (right) images. (B) SPECT analysis. (Top) Circumferential profiles of midventricular short-axis slice at rest (left) and during dobutamine infusion (right). (Bottom) Percentage SWI at rest and during dobutamine infusion.
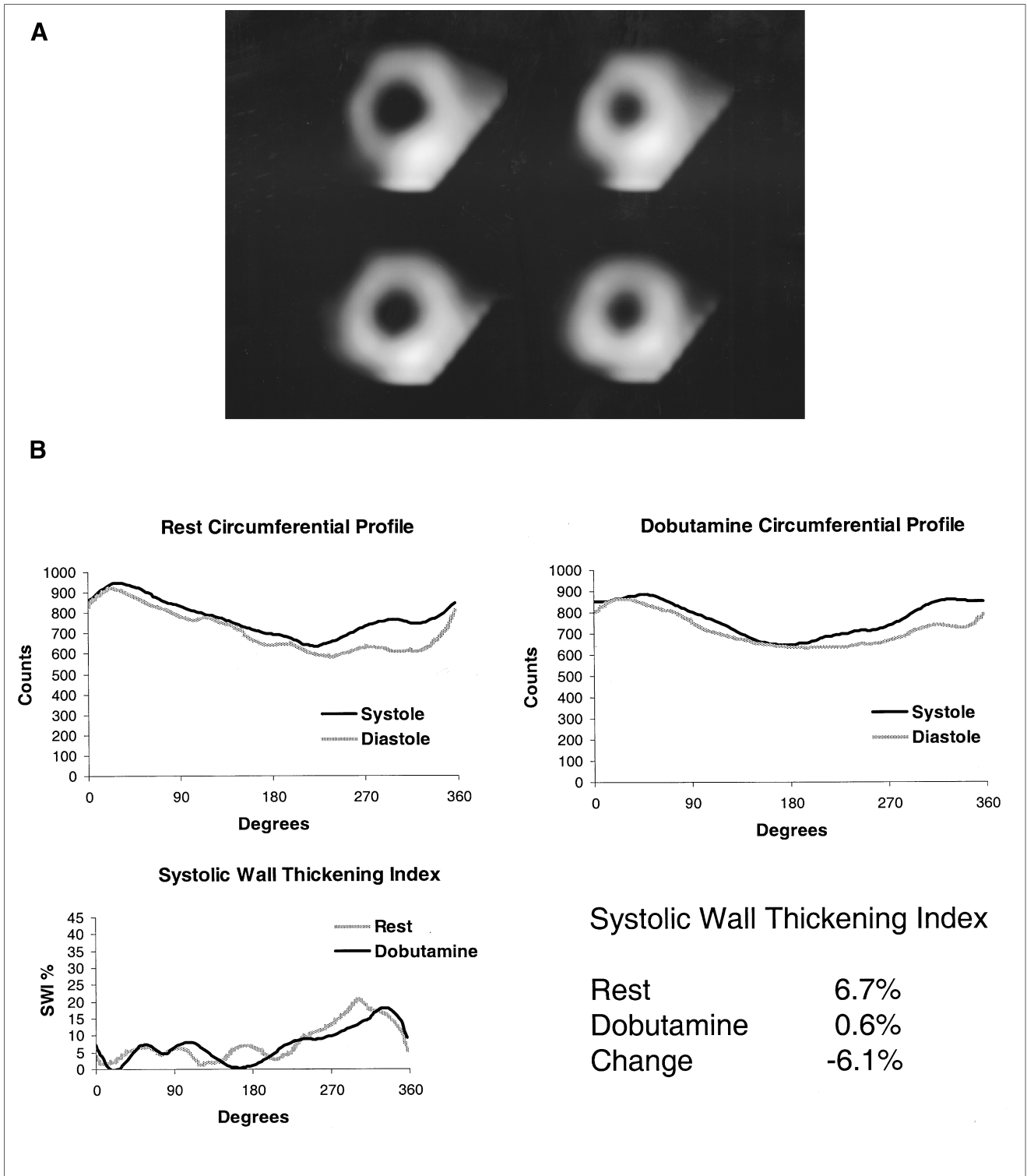
FIGURE 5.   SEMI. (A) Short-axis midventricular SPECT slices. (Top) Resting end-diastolic (left) and resting end-systolic (right) images. (Bottom) Dobutamine end-diastolic (left) and dobutamine end-systolic (right) images. (B) SPECT analysis. (Top) Circumferential profiles of midventricular short-axis slice at rest (left) and during dobutamine infusion (right). (Bottom) Percentage SWI at rest and during dobutamine infusion.
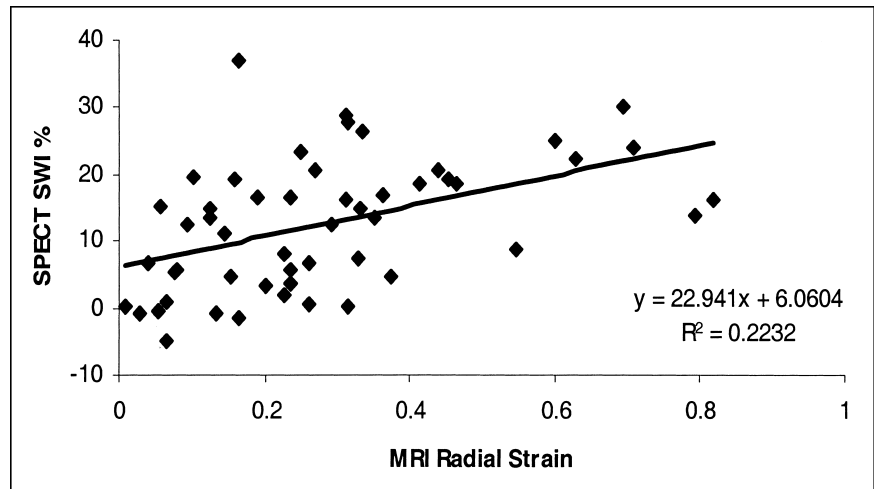
FIGURE 6. Correlation of SWI vs. MRI radial strain in anterior and anterolateral walls.

The figure shows a scatter plot with regression line:
$$y = 22.941x + 6.0604$$
$$R^2 = 0.2232$$

perfusion defect severity by scintigraphy has shown correlation with residual viable myocardium as quantified with ^{201}Tl or ^{99m}Tc-sestamibi SPECT (22,23). In a study of patients with chronic coronary artery disease who had myocardial biopsies during revascularization, the percentage of fibrosis showed an inverse correlation with resting ^{99m}Tc-sestamibi perfusion scintigraphy; however, even at the optimal threshold value for defect severity, the overall positive and negative predictive values for improvement in wall motion after revascularization were 75% and 60%, respectively (20). Other studies show similar results (1–5).

A different approach to identify myocardial viability is through evaluation of myocardial contractile reserve. Echocardiography with low-dose dobutamine may identify viable myocardium by showing an improvement in wall motion when compared with baseline function. In this study, we have shown the feasibility of simultaneously assessing perfusion and myocardial contractile reserve with gated resting ^{99m}Tc-sestamibi scintigraphy and low-dose dobutamine. Abnormal, significantly decreased wall thickening was seen at rest in stunned and subendocardial infarcted myocardium; however, during dobutamine stimulation, the stunned myocardium showed a significantly greater improvement in wall thickening compared with that in SEMI. Wall thickening in stunned myocardium during dobutamine stimulation was not significantly different from that of the normal group, as measured by SPECT SWI. Defect severity and myocardial contractile reserve were assessed simultaneously; however, contractile reserve better distinguished stunned myocardium from subendocardial infarcted myocardium in this canine model. These findings are in agreement with a previous study showing that nonviable myocardium correlates with a decreased intropic response to dobutamine (8).

Contractile reserve has shown a dependency on blood flow at rest and during dobutamine stimulation (6). A residual coronary stenosis that limits hyperemic flow will attenuate the contractile reserve response (22). On the basis of these data, one hypothesis is that radiotracer rest perfusion techniques may identify viable regions of preserved blood flow (and also decreased coronary flow reserve if combined with stress perfusion) that may not have contractile reserve by dobutamine stimulation and that complementary information regarding contractile reserve may better distinguish stunned or hibernating myocardium from a degree of SEMI that may not improve after revascularization (if the territory is not ischemic). Myocardial ischemia, identified by conventional stress and rest perfusion scintigraphy, is highly correlated with viability (7) and could potentially identify viable myocardium without contractile reserve.

A previous study of gated SPECT wall thickening and defect severity showed good sensitivity but limited specificity in predicting recovery of wall motion after revascularization of the patients (24). The addition of gated SPECT wall thickening did not significantly improve accuracy in predicting functional recovery; however, comparison with dobutamine gated SPECT to assess contractile reserve and additional stress perfusion to evaluate coronary flow reserve were not available. Gated FDG PET has also shown feasibility of identifying viability and contractile reserve (25); however, concomitant impairment of coronary flow reserve was not studied. Another gated SPECT study that evaluated patient resting [201]T1 perfusion, redistribution [201]T1, coronary flow reserve, and contractile reserve (26) showed that contractile reserve was sometimes absent in areas that were defined as hibernating and viable by perfusion scintigraphy; unfortunately, postoperative assessment of left ventricular function was not available.

Gated ^{99m}Tc-sestamibi scintigraphy, at rest and during low-dose dobutamine infusion, provides simultaneous evaluation of resting perfusion and contractile reserve. Coronary flow reserve, an important correlate of myocardial viability, can also be assessed if combined with a comparison stress perfusion scintigraphic study. In addition to the advantages of simplicity and efficiency, the exact 3-dimensional registration of perfusion and contractile reserve is likely to be

more accurate than 2-dimensional planar methods (*23*). The precise segmental characterization of coronary flow reserve, contractile reserve, and resting blood flow may improve the accuracy of identifying viable myocardium.

The SWI did not show a high correlation coefficient when compared with radial strain measurements by MRI. The SWI is derived from the relationship between the recovery coefficient and object size. This relationship is not constant over the range of possible myocardial wall thickness and, therefore, more sophisticated algorithms would be required for better correlations. The SPECT measurements of SWI are computed from data acquired and averaged over approximately 20 min; MRI radial strain is computed from analysis during a single breathhold. Changes in contractile response revealed by MRI or echocardiography may not be detected by SPECT because of the prolonged acquisition time. The sampling angle in SPECT analysis of SWI was also relatively small; therefore, the region analyzed may be slightly different in end systole compared with end diastole because of myocardial translation and rotation during contraction. This potential disadvantage was favored over the potential for lower sensitivity attributed to lower spatial resolution from a larger sampling angle. Finally, the registration of myocardial segments was by visual orientation with respect to the septum, right ventricle, apex, and base. More advanced registration techniques could improve these correlations.

The small number of canine hearts with reperfused nontransmural myocardial infarctions resulted in limited statistical power for correlations with SWI in the infarction group. This may contribute, in part, to the lack of correlation of infarct size with SWI and also for the lack of correlation of defect severity with infarct size; however, this sample size was adequate to show the feasibility of this method and to identify differences in SWI between the groups. This canine model of stunning also differs significantly from patients with viable myocardium supplied by a coronary artery with a residual stenosis. Regions of decreased coronary flow reserve may have a biphasic contractile response or negative response to dobutamine; a comparison stress myocardial perfusion study could potentially identify these regions (*7*). More delayed imaging after radiotracer injection could improve the ability to assess the inferior and inferolateral regions by allowing radiotracer clearance from the liver similar to that performed in patient studies.

The method for quantifying defect severity may also have limitations. Because the anterolateral region may be partially perfused from the left anterior descending artery, the defect severity may be underestimated because of normalizing from this region. This is an inherent difficulty in SPECT quantification that may also be present in patient studies. A single normalization region was chosen for consistency but, unfortunately, the lateral, septal, and inferior regions did not appear as better alternatives. Fortunately, the TTC staining showed minimal amount of infarct that could potentially extend into the anterolateral region.

CONCLUSION

Systolic wall thickening abnormalities may be quantified with gated ^{99m}Tc-sestamibi and contractile reserve may be assessed with low-dose dobutamine. Simultaneous assessment of resting perfusion defect severity is also possible. With dobutamine, stunned myocardium showed a significant improvement in wall thickening compared with SEMI; however, resting perfusion defect severity was not significantly different between these groups. The identification of viable myocardium in this model of stunning and SEMI was improved by assessment of contractile reserve. Evaluation of myocardial contractile reserve with resting ^{99m}Tc-sestamibi scintigraphy and low-dose dobutamine is a promising new technique to identify viable myocardium.

REFERENCES

1. Arnese M, Cornel JH, Salustri A, et al. Prediction of improvement of regional left ventricular function after surgical revascularization: a comparison of low-dose dobutamine with 201-Tl single-photon emission computed tomography. *Circulation*. 1995;91:2748–2752.

2. Vanoverschelde JL, D'Hondt AM, Marwick T, et al. Head-to-head comparison of exercise-redistribution-reinjection thallium single-photon emission computed tomography and low dose dobutamine echocardiography for prediction of reversibility of chronic left ventricular dysfunction. *J Am Coll Cardiol*. 1996;28:432–442.

3. Panza JA, Dilsizian V, Laurienzo JM, et al. Relation between thallium uptake and contractile response to dobutamine: implications regarding myocardial viability in patients with chronic coronary artery disease and left ventricular dysfunction. *Circulation*. 1995;91:990–998.

4. Qureshi U, Nagueh SF, Afridi I, et al. Dobutamine echocardiography and quantitative rest-redistribution Tl-201 tomography in myocardial hibernation: relation of contractile reserve to Tl-201 uptake and comparative prediction of recovery of function. *Circulation*. 1997;95:626–635.

5. Perrone-Filardi P, Pace L, Prastaro M, et al. Assessment of myocardial viability in patients with chronic coronary artery disease: rest-4-hour-24-hour 201-Tl tomography versus dobutamine echocardiography. *Circulation*. 1996;94:2712–2719.

6. Lee HH, Davila RV, Ludbrook PA, et al. Dependency of contractile reserve on myocardial blood flow: implications for the assessment of myocardial viability with dobutamine stress echocardiography. *Circulation*. 1997;96:2884–2891.

7. Kitsiou AN, Gopal S, Quyyumi AA, et al. Stress-induced reversible and mild-to-moderate irreversible thallium defects: are they equally accurate for predicting recovery of regional left ventricular function after revascularization? *Circulation*. 1998;98:501–508.

8. Nagueh SF, Mikati I, Weilbaecher D, et al. Relation of the contractile reserve of hibernating myocardium to myocardial structure in humans. *Circulation*. 1999;100:490–496.

9. Meza MF, Ramee S, Collins T, et al. Knowledge of perfusion and contractile reserve improves predictive value of recovery of regional myocardial function postrevascularization: a study using the combination of myocardial contrast echocardiography and dobutamine echocardiography. *Circulation*. 1997;96:3459–3465.

10. Heyman MA, Payne BD, Hoffman JI, Rudolf AM. Blood flow measurements with radionuclide-labeled particles. *Prog Cardiovasc Dis*. 1977;20:55–79.

11. O'Dell WG, Moore CC, Hunter WC, et al. Three-dimensional myocardial deformations: calculation with displacement field fitting to tagged MR images. *Radiology*. 1995;195:829–835.

12. Moore CC, McVeigh ER, Zerhouni EA, et al. Noninvasive measurement of three-dimensional myocardial deformation with tagged magnetic resonance imaging during graded local ischemia. *J Cardiovasc Magn Reson*. 1999;1:207–222.

13. Yamashita K, Tamaki N, Yonekura Y, et al. Quantitative analysis of regional wall motion by gated myocardial positron emission tomography: validation and comparison with left ventriculography. *J Nucl Med*. 1989;30:1775–1786.

14. Pagley PR, Beller GA, Watson DD, et al. Improved outcome after coronary bypass surgery in patients with ischemic cardiomyopathy and residual myocardial viability. *Circulation*. 1997;96:793–800.

15. Beanlands RS, Hendry PJ, Masters RG, et al. Delay in revascularization is associated with increased mortality rate in patients with severe left ventricular dysfunction and viable myocardium on fluorine18-fluorodeoxyglucose positron emission tomography imaging. *Circulation*. 1998;98(suppl):II51–II56.

16. Picano E, Sicari R, Landi P, et al. Prognostic value of myocardial viability in medically treated patients with global left ventricular dysfunction early after an acute uncomplicated myocardial infarction: a dobutamine stress echocardiographic study. *Circulation*. 1998;98:1078–1084.

17. Afridi I, Kleiman NS, Raizner AE, Zoghbi WA. Dobutamine echocardiography in myocardial hibernation: optimal dose and accuracy in predicting recovery of ventricular function after coronary angioplasty. *Circulation*. 1995;91:663–670.

18. Gunning MG, Anagnostopoulos C, Knight CJ, et al. Comparison of Tl-201, Tc99m tetrofosmin, and dobutamine magnetic resonance imaging for identifying hibernating myocardium. *Circulation*. 1998;98:1869–1874.

19. Parodi P, Schelbert HR, Schwaiger M, et al. Cardiac emission computed tomography: underestimation of regional tracer concentrations due to wall motion abnormalities. *J Comput Assist Tomogr*. 1984;8:1083–1092.

20. Dakik HA, Howell JF, Lawrie GM, et al. Assessment of myocardial viability with ^{99m}Tc-sestamibi tomography before coronary bypass graft surgery: correlation with histopathology and postoperative improvement in cardiac function. *Circulation*. 1997;96:2892–2898.

21. Dilsizian V, Arrighi JA, Diodati JG, et al. Myocardial viability in patients with chronic coronary artery disease: comparison of ^{99m}Tc-sestamibi with thallium reinjection and [^{18}F]fluorodeoxyglucose. *Circulation*. 1994;89:578–587.

22. Chen C, Li L, Chen LL, et al. Incremental doses of dobutamine induce a biphasic response in dysfunctional left ventricular regions subtending coronary stenoses. *Circulation*. 1995;92:756–766.

23. Nagel E, Lehmkuhl HB, Klein C, et al. Noninvasive diagnosis of ischemia-induced wall motion abnormalities with the use of high-dose dobutamine stress MRI: comparison with dobutamine stress echocardiography. *Circulation*. 1999; 99:763–770.

24. Stollfuss JC, Haas F, Matsunari I, et al. ^{99m}Tc-Tetrofosmin SPECT for prediction of functional recovery defined by MRI in patients with severe left ventricular dysfunction: additional value of gated SPECT. *J Nucl Med*. 1999;40:1824–1831.

25. Yamagishi H, Akioka K, Hirata K, et al. Dobutamine-stress electrocardiographically gated positron emission tomography for detection of viable but dysfunctional myocardium. *J Nucl Cardiol*. 1999;6:626–632.

26. Narula J, Dawson MS, Singh BK, et al. Noninvasive characterization of stunned, hibernating, remodeled and nonviable myocardium in ischemic cardiomyopathy. *J Am Coll Cardiol*. 2000;36:1913–1919.